LAUNCH VEHICLE PERFORMANCE ENHANCEMENT USING AERODYNAMIC ASSIST

Except where reference is made to the work of others, the work described in this thesis is my own or was done in collaboration with my advisory committee. This thesis does not include proprietary or classified information.

_____
Brian Robert McDavid

Certificate of Approval:

_____	_____
John E. Burkhalter Professor Emeritus Aerospace Engineering	Roy J. Hartfield, Jr. Chair Professor Aerospace Engineering
_____	_____
Brian Thurow Assistant Professor Aerospace Engineering	George T. Flowers Dean Graduate School

LAUNCH VEHICLE PERFORMANCE ENHANCEMENT USING AERODYNAMIC ASSIST

Brian Robert McDavid

A Thesis

Submitted to

the Graduate Faculty of

Auburn University

in Partial Fulfillment of the

Requirements for the

Degree of

Master of Science

Auburn, Alabama
August 9th, 2008

LAUNCH VEHICLE PERFORMANCE ENHANCEMENT USING AERODYNAMIC ASSIST

Brian Robert McDavid

Permission is granted to Auburn University to make copies of this thesis at its discretion, upon request of individuals or institutions and at their expense. The author reserves all publication rights

_____

Signature of Author

_____

Date of Graduation

VITA

Brian Robert McDavid was born on September 14th, 1982, in Brunswick, Maine to Harry and Leslie McDavid. He graduated from Bob Jones High School in Madison, Alabama and began attending Auburn University in 2001. As an undergraduate, he was inducted into the Aerospace Engineering Honor Society Sigma Gamma Tau and the national engineering honor society of Tau Beta Pi. Brian graduated Cum Laude in May 2006 with a Bachelor of Aerospace Engineering degree. He entered the Auburn University Graduate School in Fall 2006 to pursue a Master of Science degree in Aerospace Engineering. On December 29th, 2006, Brian married his beautiful wife Nicole (Cann) McDavid.

THESIS ABSTRACT

LAUNCH VEHICLE PERFORMANCE ENHANCEMENT USING AERODYNAMIC ASSIST

Brian Robert McDavid

Master of Science, August 9 2008
(B.A.E., Auburn University, 2006)

66 Typed Pages

Directed by Roy J. Hartfield, Jr.

A complete preliminary design model of a three-stage solid-fuel launch vehicle has been combined with a genetic algorithm to perform an optimization study with the goal to enhance performance using aerodynamic assist. Three studies have been completed which include improving the suborbital and orbital flights of a modern intercontinental ballistic missile and improving on the orbital flight of a generic three-stage launch vehicle. The performance is enhanced by varying the geometric definition of the attached wing structure and the internal propellant geometry while the external geometry remains constant. Initial system weights and propellant mass fractions were found to decrease with the addition of the wing structure. Further enhancement involves a payload increase by 10% with a negligible increase in system weight, and a propellant mass decrease by 5.2% without impairing the flight performance.

ACKNOWLEDGEMENTS

The author would like to thank Dr. Roy Hartfield and Dr. John Burkhalter for their technical and professional guidance and support. The author also would like to thank Dr. Murray Anderson, the author of the 3.1 IMPROVE Genetic Algorithm, without which this thesis would not have been possible. The author would also like to thank his parents Harry and Leslie and sister Amanda for their support and encouragement, and his wife Nicole for all her patience and support provided throughout the graduate school process.

Style manual of journal used

The American Institute of Aeronautics and Astronautics Journal

Computer software used

Improve 3.1 Genetic Algorithm, Tecplot 10, Compaq Visual Fortran, Microsoft Excel, Microsoft Word

TABLE OF CONTENTS

LIST OF TABLES ix

LIST OF FIGURES x

NOMENCLATURE xii

1.0 INTRODUCTION 1

2.0 MODEL BACKGROUND 3

2.1 GENETIC ALGORITHM 3

2.2 ADVANTAGES OF THE GENETIC ALGORITHM 5

2.3 PRELIMINARY DESIGN MODEL 8

2.3.1 OBJECTIVE FUNCTION AND GA INITIALIZATION 9

2.3.2 DESIGN AND MISSION PARAMETERS 11

2.3.3 PREDICTIVE MODEL 15

3.0 VALIDATION 23

4.0 AERODYNAMIC PERFORMANCE ENHANCEMENT 27

4.1 MINUTEMAN-III SUBORBITAL ENHANCEMENT 29

4.1.1 SUBORBITAL IMPROVEMENT 31

4.1.2 ORBITAL IMPROVEMENT 39

4.2 THREE-STAGE ORBITAL ENHANCEMENT 43

5.0 SUMMARY 47

REFERENCES 49

LIST OF TABLES

Table 1: GA Design Variables for Minuteman-III 12

Table 2: Constant Mission Parameters 13

Table 3: Propellant Design Variables 13

Table 4: Wing and Tail Design Parameters 14

Table 5: Minuteman-III Parameters 14

Table 6: Mass Property Components 22

Table 7: Minuteman-III Validation 24

Table 8: PBAA/AP/Al Characteristics (English Units) 26

Table 9: MM3 Suborbital Enhancement 38

Table 10: MM3 Suborbital Mass Fractions 38

Table 11: MM3 Orbital Enhancement 43

Table 12: MM3 Orbital Mass Fractions 43

Table 13: Generic Three-Stage Orbital Enhancement 46

Table 14: Generic Three-Stage Mass Fractions 46

LIST OF FIGURES

Figure 1: Tournament Algorithm 4

Figure 2: Crossover 7

Figure 3: Mutation 8

Figure 4: Optimization Model Outline 10

Figure 5: GA Population and Generation Setup 12

Figure 6: Bell Nozzle Schematic[30] 18

Figure 7: Circular Arc Airfoil[30] 20

Figure 8: Minuteman-III Validation Model 25

Figure 9: Air Density vs. Altitude 27

Figure 10: Minuteman-III Dynamic Pressure 28

Figure 11: Minuteman-III 30

Figure 12: Minuteman-III with 2540 Payload 31

Figure 13: Altitude vs. Time (MM3-Wings) 33

Figure 14: Thrust vs. Time (MM3-Wings) 33

Figure 15: Weight vs. Time (MM3-Wings) 34

Figure 16: GA Best Answer Convergence 34

Figure 17: Vehicle Diagram (MM3-Reduced Propellant) 36

Figure 18: Convergence for MM3-Reduced Propellant 36

Figure 19: Vehicle Diagram (MM3-Increased Payload) 37

Figure 20: Orbital MM3 GA Convergence 40
Figure 21: Orbital MM3 Wings 41
Figure 22: Orbital MM3 Altitude vs. Time 41
Figure 23: Orbital MM3 Thrust Profile 42
Figure 24: Orbital MM3 Convergence History 42
Figure 25: Generic Three-Stage Vehicle 44
Figure 26: Three-Stage Altitude vs. Time 45
Figure 27: Three-Stage Thrust Profile 45

NOMENCLATURE

$\dot{m}$	Mass Flow Rate
GA	Genetic Algorithm
r	Propellant Burning Rate
a	Empirical Constant
n	Burning Rate Index
P_c	Chamber Pressure
P_e	Exit Pressure
P_a	Ambient Pressure
A_b	Burning Area
ρ_b	Solid Propellant Density
c^*	Characteristic Velocity
R	Specific Gas Constant
γ	Specific Heat Ratio
T_c	Chamber Temperature
A^*	Throat Area
u_e	Exit Velocity
T	Thrust
L_f	Fractional Nozzle Length
MW	Molecular Weight
MM3	Minuteman-III
rpvar	Propellant Outer Radius
rivar	Propellant Inner Radius
fvar	Fillet Radius Ratio
eps	Epsilon Star Width
ptang	Star Point Angle
fn	Fractional Nozzle Length Ratio
diath	Throat Diameter
rnose	Nose Radius Ratio
thet0	Initial Launch Angle
b2tdb	Tail Semi Span
crtdb	Tail Root Chord Length
trt	Taper Ratio Tail
tLEswp	Sweep of Leading Edge in Tail Fins
xTEtl	Distance to Leading Edge of Tail Fins
b2wdb	Wing Semi Span
crwdb	Wing Root Chord Length
trw	Taper Ratio Wing

wLEswe	Sweep of Leading Edge in Wings
xLEw	Distance to Leading Edge of Wings

1.0 INTRODUCTION

During the development of the Space Shuttle, the orbiter was designed with wings which were anticipated for use only during reentry. The initial proposal for launch was essentially a gravity turn launch which did not make use of lifting aerodynamics. During the design process, launch studies were being conducted by Woltosz[1,2] to ascertain the most advantageous launch trajectory using a tool known as Rocket Ascent G-limited Moment-balanced Optimization Program (RAGMOP). During this optimization exercise, it was discovered that an "upside down" launch to orbit could increase payload by 20% (about 8,000 lb at the time) [1,2]. The reason for this improvement involved the more efficient use of the orbiter wings for lift production in the upside down configuration during the atmospheric portion of the ascent.

The payload advantage gained by the change in the ascent trajectory was entirely free structurally for the Space Shuttle; however, based on the marked improvement in performance associated with aerodynamic lifting for the shuttle, it is possible that substantial improvement in net payload to orbit could be obtained for current launch vehicles using aerodynamic lifting during the first stage burn despite the cost of adding some mass in the form of wing structure (to the first stage). The potential payoff with regard to achieving additional payload to orbit warrants the investigation described herein which makes use of preliminary design level modeling and optimization tools. This study includes physical modeling of the system components and digitally flying the launch

vehicle fitted with candidate wing design configurations through candidate ascent trajectories. Using this general approach to preliminary design, researchers at Auburn University have demonstrated substantial performance improvement for a Minotaur-type vehicle using preliminary design level tools and a genetic algorithm[3]. The current investigation uses the same preliminary design tools and includes wings to explore the viability of the concept of using aerodynamic lifting during first phase ascent for a generic vehicle. Two optimization studies have been completed for this thesis with the goal of maximizing payload to orbit. The first study was conducted while changing only the geometric definition of the add-on wing configuration (semi-span, root chord, tip chord, sweep angle, taper ratio, and position). The first study includes a suborbital optimization and an orbital optimization. The second study optimized an orbital launch vehicle similar to the Minuteman-III from the "ground-up".

The vehicle configuration for both studies uses a three-stage solid-fuel propulsion system. The published fuel for the Minuteman-III is polybutadiene-acrylic acid with ammonium perchlorate and aluminum (PBAA/AP/Al). PBAA has been hardwired in the model as the propellant selection for every study in this thesis to ensure that performance gains are associated with the geometric design and aerodynamics rather than with propellant characteristics. Higher overall performance is expected from launch vehicles which incorporate advanced design optimization methods, aerodynamic lifting and advanced propellant chemistry. The propellant choice is fixed, but the grain geometry is selected by the genetic algorithm.

2.0 MODEL BACKGROUND

2.1 GENETIC ALGORITHM

Genetic algorithms (GAs) are a powerful class of evolutionary computing tools in which elements from biology such as reproduction, inheritance, mutation, selection, and fitness, are used to solve very complex problems in a wide range of applications. John Holland presented the method of applying the evolutionary process to solve scientific, mathematical, and engineering problems in his 1975 book *Adaptation in Natural and Artificial Systems*[4]. The benefits of using a GA to design and optimize a model in a set design space have been well documented. A few specific aerospace applications include the design and optimization of propellers[5], freight truck aerodynamics[6], wings and airfoils[7,8,9,10], rockets[11,12], missiles[13,14,15,16,17,18], flight trajectories[19], spacecraft controls[20,21], and turbines[22,23,24].

Genetic algorithms find an optimized solution by breeding new sets of data (*members*) over a defined number of generations. The process starts by randomly creating the first set of members based on a user specified design space. The user constricts the minimum and maximum values for each design parameter. Each individual member is a possible solution to the problem. Koza[25], who worked with Holland to pioneer the first batch of GAs, states that the genetic algorithm transforms a *population* (set) of individuals (or members), each with an associated *fitness* value, into a new *generation* of

the population using reproduction, crossover, and mutation. Specifically, each member is analyzed by the performance codes of the design model, and a fitness is assigned to each member based on how well the member's performance matched the objective function. The final solution is the member that has the best fitness at the end of the last generation.

The genetic algorithm used in this effort is the IMPROVE© code, or Implicit Multi-Objective PaRameter Optimization Via Evolution, and was developed by Anderson[26]. The IMPROVE© code is a binary encoded *tournament* based genetic algorithm. The tournament nomenclature refers to the method employed to create the members of the new population, and it involves three basic steps. Figure 1 summarizes the tournament algorithm.

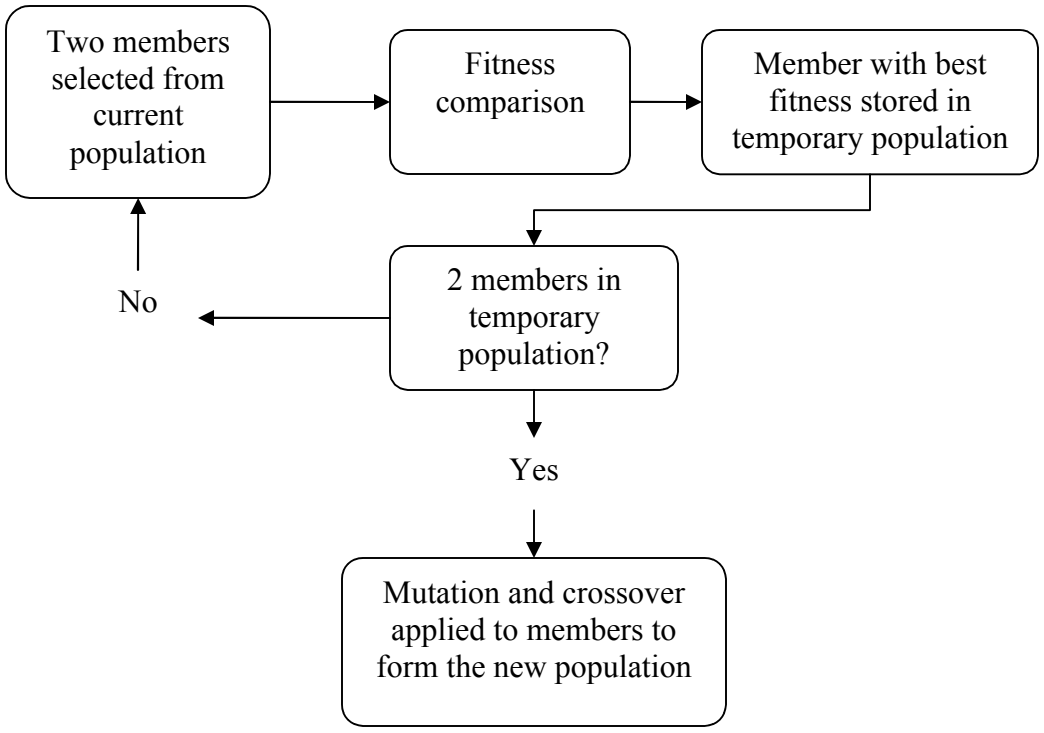

Figure 1: Tournament Algorithm

First, two members of the current population are selected at random and their fitness values are compared. The member having the better fitness moves to a temporary population, and the other goes back to the current population. The process repeats to generate a two member temporary population. Mutation and crossover operations are performed on the two members in the temporary population, creating two new members which are placed into the new population. This process continues until the new population is filled with the correct number of members. The tournament method therefore creates a new population with members having characteristics, or heredity, from the previous population but in different combinations which may result in improved fitness.

In addition to generating the members of the new population via tournament, *elitism* is employed. Elitism takes the best performing member of the current population and moves it to the next population without changing it at all. This is to safe-guard against the mutated members all performing worse than the best member of the previous population and sending the GA backwards. Elitism and tournament selection ensure that the GA will find solutions that continually approach the target fitness. It should be noted that the use of elitism, particularly with small populations can materially reduce the genetic diversity of the population and care should be taken to address the adequacy of the population size when using this option.

2.2 ADVANTAGES OF THE GENETIC ALGORITHM

There are several reasons why the genetic algorithm was chosen for this effort instead of a gradient marching method. Gradient methods march toward a local

maximum or minimum by taking small steps that are proportional to the gradient of the function. This requires that the objective function be differentiable in every independent variable. If the function is not completely differentiable, then a singularity will develop and the ability of the routine to march towards a maximum or minimum will be ruined. In many systems it is impossible for the objective function to be completely differentiable. For example, propellant type is not differentiable. A second problem with gradient methods is that convergence to local optima is more common in design spaces with many variables. The current preliminary design model requires 37 parameters, and their derivatives are not easily ascertained. While the GA has a greater likelihood finding a global optimum solution, obtaining this solution is not guaranteed. However, recent techniques such as mutation and crossover help the GA to approach the global solution.

Mutation and crossover are powerful tools that help prevent genetic algorithms from becoming stuck in a local optimum. A design variable is represented in the IMPROVE© genetic algorithm by a binary string such as 101100101. When the tournament selects two members to move to the next population, crossover is one of the methods used to produce the new member, or *offspring*. The IMPROVE© code uses single point crossover. In single point crossover, a location is chosen in the binary string of each parent, and the remaining *alleles* are swapped from one parent to the other. Crossover is more easily described by looking at a simple one offspring example as shown in Figure 2. The numbers in bold are the values transferred to the offspring.

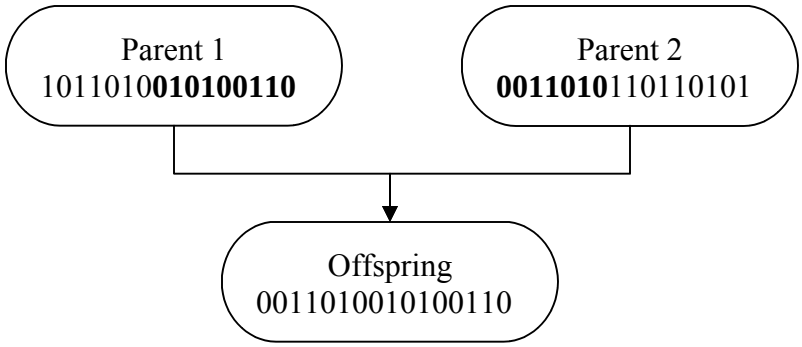

Figure 2: Crossover

When crossover is applied, the offspring takes one section of each parent's genes. The point at which the parent string is broken depends on the randomly selected crossover point. Crossover occurrence is based on a set probability within the genetic algorithm setup file, so sometimes the parent is directly copied to the offspring.

The second function that the genetic algorithm employs is mutation. After the tournament selection and crossover, some of the offspring has been copied directly from the parents, and the others have been affected by crossover. In order to ensure genetic diversity, a small chance allowed for mutation is allowed. Each variable in the model is represented by a binary string. The 1s and 0s that form a binary string are called alleles. All of the members and their alleles are looped through, and if the allele is selected for mutation, it is either changed by a small amount or replaced with a new value. Figure 3 shows an example of mutation. The allele in bold has been chosen for mutation and the result is a change from a 0 to a 1.

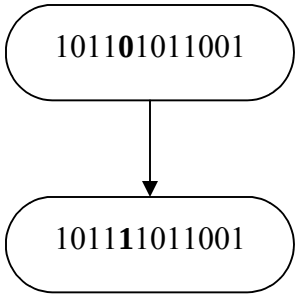

Figure 3: Mutation

If the GA approaches a local solution, this random change is very useful because it very often creates a new member that is an improvement and can escape the trap of a local solution.

2.3 PRELIMINARY DESIGN MODEL

As can be seen from References [5-24], the genetic algorithm is effective at optimizing a problem when paired with a capable predictive model. The model in this effort is a suite of FORTRAN codes used to model and simulate the flight of a three-stage solid fueled rocket. The model was developed by Jenkins, Hartfield, and Burkhalter[15], and was modified to include orbital trajectories by Bayley[3]. These codes accurately predict and simulate the performance of a three-stage solid fueled rocket by modeling the aerodynamics, mass properties, and propulsion. The six-degree of freedom code manages all the other codes while it simulates the flight of the missile and updates the performance characteristics synchronized in time. This approach and this particular model was validated by Bayley using the Minotaur as a baseline for comparison.

2.3.1 OBJECTIVE FUNCTION AND GA INITIALIZATION

The results of the flight are used to determine the fitness (or how well the member met the desired optimization goals). The fitness is calculated by sending the appropriate performance values into the objective function, with the output being the fitness. In this model, the objective function is a quantitative measure that the GA uses to determine which members have better performance. Two of the objective functions for this model are to match a user specified orbital altitude and orbital velocity. These specified values are chosen before the GA is started. After each member is digitally flown through the model, values for the orbital altitude and velocity are obtained. Since two of the goals are to match these values, the objective function compares the obtained value to the desired value by using equations 1 and 2.

$$answer\ 1 = \frac{|alt1 - altorb|}{altorb} \tag{1}$$

$$answer\ 2 = \frac{|v1 - vorb|}{vorb} \tag{2}$$

If these were the only two desired goals, the fitness would be

$$fitness = answer\ 1 + answer\ 2 \tag{3}$$

In order to reach the desired altitude and velocity, answer 1 and answer 2 must be minimized. As answer 1 approaches zero, the actual altitude becomes closer to the desired altitude. Therefore, the member with the smallest value for the fitness is the best performing member of the population and its characteristics are carried over into the next generation. A second method of determining the fitness, pareto, could be used instead of equation 3. Pareto style optimization separates the goals and attempts to minimize each

answer individually instead of the combined answer. Pareto was not used for the studies in this thesis.

Figure 4 shows a very simplified and basic outline of the model code structure. The first step in the optimization model is the initialization of the genetic algorithm. One benefit of the GA is that it does not need an initial starting point. Instead, the GA reads an input file created by the user which specifies the *design space* or range (minimum, maximum, and resolution) for each design variable and the GA creates an initial population by randomly selecting the values for each design parameter. The GA is binary encoded and the values in the design space determine the number of bits required to adequately represent each parameter by equation 4.

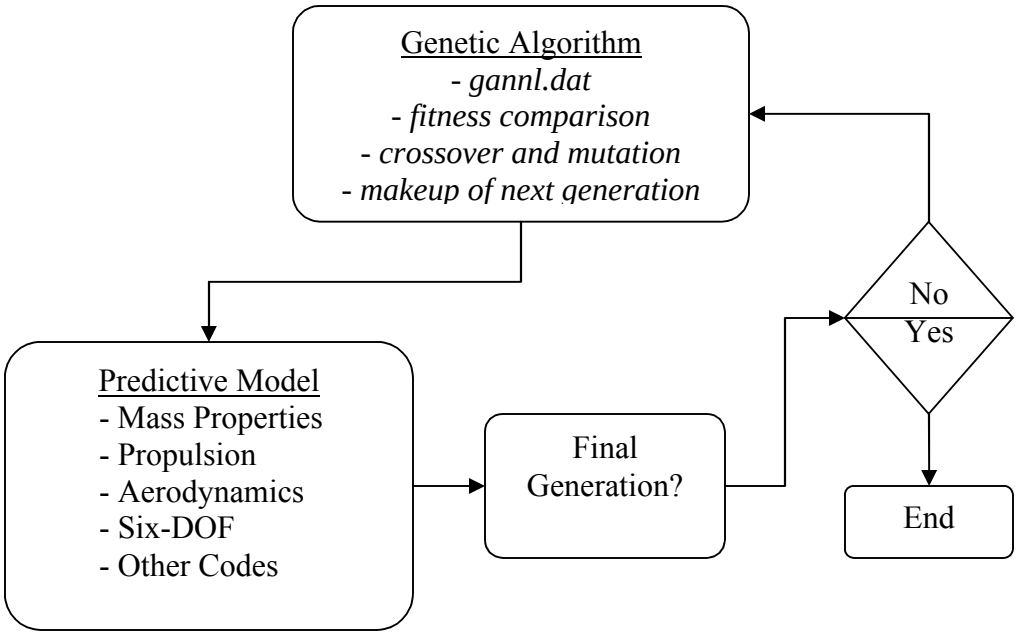

Figure 4: Optimization Model Outline

$$nbits = \frac{\ln\left(\frac{\max - \min}{resolution}\right)}{\ln(2)} + 1 \qquad (4)$$

The variables in equation 4 are discussed in section 2.3.2. The number of bits required for each parameter is important because the total number of bits influences the recommended population size (n) by

$$n = (3.0)\, nbits \qquad (5)$$

A large population size is usually needed for a complicated design problem with a large design space. The maximum population size that the IMPROVE© code can use is set at 400. The recommended number of generations is not as explicitly defined; however a larger number of generations is more likely to produce an optimum solution. The trade-off is that a large number of generations and a large population size can lead to significant computer run times. It is up to the user to determine the appropriate number of generations and to ascertain whether the solution produced is adequate.

2.3.2 DESIGN AND MISSION PARAMETERS

A section of the *gannl.dat* setup file used for this study is seen in Table 1. Figure 5 shows a section from the setup file that the GA reads to set the number of populations and generations. Table 1 and Figure 5 show how the GA reads the design variables and how the maximum, minimum, resolution, size of the population, and number of generations are specified. The first column is a truncated description of the design variable name, followed by the maximum, minimum, and resolution values. The population size and number of generations are listed at the end.

Table 1: GA Design Variables for Minuteman-III

Parameter	Maximum	Minimum	Resolution
rpvar1	0.8000	0.2000	0.0100
rivar1	0.9900	0.0100	0.0100
fvar1	0.2000	0.0100	0.0100
eps1	0.9700	0.1000	0.1000
ptang1	50.0000	10.0000	1.0000
fn1	0.9900	0.6000	0.0100
diath1	35.0000	5.0000	0.1000
rpvar2	0.8000	0.2000	0.0100
rivar2	0.9900	0.0100	0.0100
fvar2	0.2000	0.0100	0.0100
eps2	0.9700	0.5000	0.1000
ptang2	50.0000	10.0000	0.1000
fn2	0.9900	0.6000	0.0100
diath2	35.0000	5.0000	0.1000
rpvar3	0.8000	0.2000	0.0100
rivar3	0.9900	0.0100	0.0100
fvar3	0.2000	0.0100	0.0100
eps3	0.9700	0.5000	0.1000
ptang3	50.0000	10.0000	0.1000
fn3	0.9900	0.6000	0.0100
diath3	35.0000	5.0000	0.1000
rnose	0.7500	0.5000	0.0100
thet0	89.0000	70.0000	1.0000
b2tdb	1.4000	0.1000	0.1000
crtdb	1.2000	0.1000	0.1000
trt	0.9900	0.5000	0.0100
tLEswp	25.0000	5.0000	0.1000
xTEtl	0.9900	0.5000	0.1000
dele0	15.0000	0.0000	0.1000
timeb1	7.0000	0.1000	0.1000
timeb2	35.0000	7.0000	0.1000
timeee	90.0000	15.0000	1.0000
b2wdb	1.5000	0.1000	0.1000
crwdb	1.2000	0.1000	0.1000
trw	0.9900	0.5000	0.1000
wLEswe	25.0000	5.0000	0.1000
xLEw	0.6500	0.0500	0.1000

```
1      ; ifreq
400    ; mempops
300    ; maxgen
```

Figure 5: GA Population and Generation Setup

The launch location must be specified in order to accurately simulate an orbital trajectory. Table 2 lists four mission parameters that are constant among all the different optimization cases.

Table 2: Constant Mission Parameters

Launch Site	Vandenberg AFB, CA (34.6° N, 120.6° W)
Launch Direction	Due North (0° Azimuth or i = 90°/polar orbit)
Desired Orbital Velocity	22,000 ft/s
Desired Orbital Altitude	750,000 ft

The desired system mass is another important mission parameter, however the appropriate value is different based on which optimization case is being considered. For example, the validation of the Minuteman-III has a desired system mass of 79,432 lbm, whereas in cases where the wings are employed to reduce required propellant mass through aerodynamic lifting the desired system mass is smaller. These are discussed in more detail in the appropriate section of this thesis.

The optimization starts with the GA generating a set of 37 design parameters to describe the launch vehicle. The geometric variables that describe the propellant for each stage, as well as two external variables are shown in Table 3.

Table 3: Propellant Design Variables

Stages 1, 2, and 3	**GA Variable**
Propellant Outer Radius Ratio	rpvar
Propellant Inner Radius Ratio	rivar
Fillet Radius Ratio	fvar
Epsilon Star Width	eps
Star Point Angle	ptang
Fractional Nozzle Length Ratio	fn
Throat Diameter	diath
Other	
Nose Radius Ratio	rnose
Initial Launch Angle	thet0

Five variables are required to describe the wings/tails as seen in Table 4. All geometric variables are non-dimensionalized by the body diameter.

Table 4: Wing and Tail Design Parameters

Wings/Tails	GA Variable
Semispan	b2wdb / b2tdb
Root Chord	crwdb / crtdb
Taper Ratio	trw / trt
Leading Edge Sweep Angle	wLEswe / tLEswp
Leading Edge Location	xLEw / tLEtl

The first study takes the Minuteman-III missile and attempts to increase the payload/reduce the propellant weight, therefore certain external geometric parameters are hardwired into the predictive model based on Minuteman-III data. These parameters are shown in Table 5. The payload is the only parameter that changes in some of the optimization cases. The second study does not constrain the vehicle to match the Minuteman-III values, therefore the only value hardwired into the model is the stage propellant.

Table 5: Minuteman-III Parameters

Parameter	Minuteman-III Value
Payload*	2,540 lbm
Stage 1 Length	295.20 in
Stage 1 Diameter	66.00 in
Stage 1 Propellant	PBAA/AP/Al
Stage 2 Length	184.00 in
Stage 2 Diameter	52.00 in
Stage 2 Propellant	PBAA/AP/Al
Stage 3 Length	90.00 in
Stage 3 Diameter	52.00 in
Stage 3 Propellant	PBAA/AP/Al

Constants such as material densities, program limits, target location, and physical constants such as the radius of the earth are contained in a file called *YYvar.dat*. These values can be changed easily if necessary to support new data.

2.3.3 PREDICTIVE MODEL

Propulsion

The propulsion code is the first to be called after the genetic algorithm is initialized. This model analyzes the basic thrust performance and creates a full sea-level thrust profile. Since the vehicle in this effort is three stages, the propulsion model is called three times and the propulsion characteristics are determined for each stage separately and in sequence. The basic theory in this model assumes steady-state operation, which requires that the mass produced by the burning propellant is equal to the mass output through the nozzle. Detailed derivations of the equations presented here can be found in Sutton[27]. The burning rate is modeled by the empirical equation

$$r = ap_c^n \tag{6}$$

where a is an empirical constant, n is the burning rate index, and P_c is the chamber pressure. The mass flow rate of hot gas generated by the burning propellant and flowing away from the motor is given by

$$\dot{m} = A_b r \rho_b \tag{7}$$

where A_b is the burning area of the propellant grain, and ρ_b is the solid propellant density prior to the motor start.

The burning area of the propellant can be tedious to calculate by hand, but computers have made this process much simpler. Star grains and wagon wheel grains are considered for this vehicle. The star and wagon wheel equations have been extensively developed by Barrere[34] and reviewed by Hartfield[29]. It is important to note that the maximum burn area corresponds to the maximum chamber pressure, and for a star grain

the maximum burn area will always occur at the beginning of the burn or at the end of phase II. Due to this fact, an initial check on chamber pressure is done once a design is determined so that the thickness of the can be determined and a precise estimate of the case weight can be calculated.

Isentropic flow is assumed through the nozzle, and the characteristic velocity is defined as

$$c^* = \sqrt{\frac{RT_c}{\gamma}}\left(\frac{\gamma+1}{2}\right)^{\frac{\gamma+1}{2(\gamma-1)}} \tag{8}$$

where T_c is the chamber temperature and gamma is defined by the propellant.

The relationships of isentropic flow can be used to express the mass flow rate through the nozzle as

$$\dot{m} = \frac{p_c A^* \sqrt{\gamma}}{\sqrt{RT_c}}\left(\frac{2}{\gamma+1}\right)^{\frac{\lambda+1}{2(\gamma-1)}} \tag{9}$$

$$\dot{m} = \frac{p_c A^*}{c^*} \tag{10}$$

where p_c is the chamber pressure, A* is the throat area, R is the specific gas constant, T_c is the chamber temperature, gamma is the specific heat ratio, and c* is the characteristic velocity.

The chamber pressure can be expressed by

$$P_c = \left(\frac{A_b}{A_t} a \rho_b c^*\right)^{\frac{1}{1-n}} \tag{11}$$

Assuming adiabatic, steady, 1-D flow, the exit velocity is

$$u_e = \sqrt{\frac{2\gamma RT_c}{\gamma - 1}\left(1 - \left(\frac{P_e}{P_c}\right)^{\frac{\gamma}{\gamma - 1}}\right)} \tag{12}$$

The thrust of the rocket motor is finally determined by

$$T = \dot{m}u_e + A_e\left(P_e - P_a\right) \tag{13}$$

A bell shaped nozzle is employed for this model because it is desirable to have a nozzle that is minimum weight while not sacrificing performance. The geometric design of the nozzle has been taken from Ref. 16 and Ref. 30. If a conical nozzle is used for comparison, then the relative performance and relative weight can be determined. The conical nozzle is a 15 degree half cone with a given expansion ratio and throat diameter. The bell nozzle has the same expansion ratio and throat diameter, but the mass is significantly lower. The length of the bell nozzle can be determined from equation 14, where L_f is the fractional nozzle length and the denominator is the equivalent known conical nozzle length.

$$L_f = \frac{L_{bell}}{L_{15^\circ - cone}} \tag{14}$$

The bell nozzle diagram is shown in Figure 6.

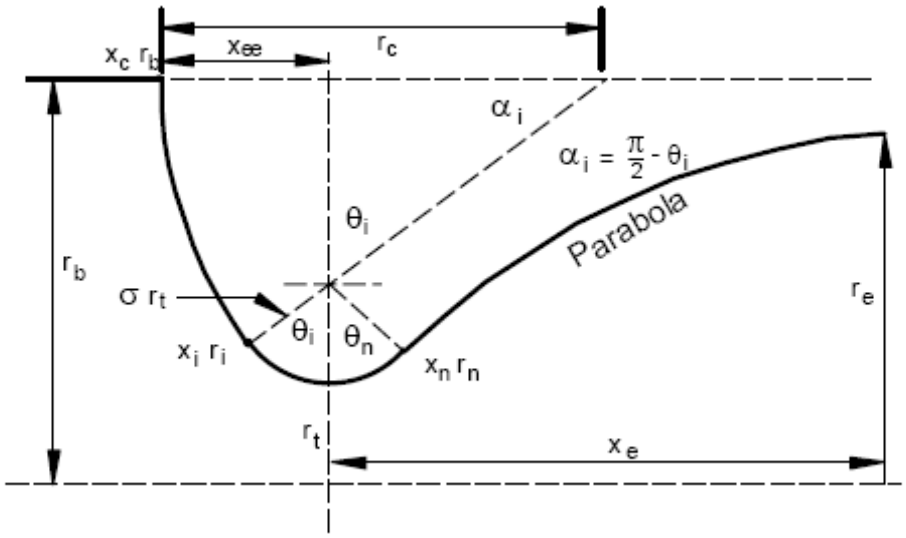

Figure 6: Bell Nozzle Schematic[30]

Huzel and Huang[35] contains a detailed correlation to the bell nozzle performance equations, as derived from the method of characteristics solutions. These curves are interpolated in the nozzle model to predict a shape and corresponding performance for any set of design parameters. The geometric performance of the bell nozzle is a few percent higher than the conical nozzle for all expansion ratios and length fractions. The expansion ratio of the nozzle is limited to the body diameter.

Aerodynamics Model

The aerodynamics model is performed by Aerodsn, which is a fast predictor aerodynamics code and has been used successfully in all of the missile optimization codes at Auburn University for contracts with the U.S. Army, Missile and Space Intelligence Center, and the U.S. Air Force. Aerodsn is non-linear and assumes that there are no boundary layers, that no separation occurs, and that the vehicle is axis-symmetric. Some improvements in Aerodsn have been incorporated, such as the modeling of a

variable body diameter. More accurate computational fluid dynamic (CFD) simulations are available; however the high computational cost makes CFD an unreasonable choice for genetic algorithm applications where thousands of missiles are simulated under a broad range of flight conditions.

Aerodsn generates aerodynamic databases based on the vehicle geometry and other necessary parameters. Empirical curve fits of wind tunnel data are performed and aerodynamic constants are determined over a wide range of flow conditions. The vehicle geometry, initial constants, and empirical data are combined to generate an aerodynamic database to describe the flight conditions. Aerodsn can model either a cone or an ogive shape for the nosecone and assumes the body is cylindrical in shape; this study uses an ogive nosecone. The vehicle is smooth except for the first stage which contains the wing and tail set. The four canards and four tail fins are set in a "+" configuration on the first stage. The wing and tail locations on the first stage are GA variables. Vehicles with different wing configurations are not analyzed because Aerodsn only allows for the cruciform configuration for the wings and tails. Aerodsn also limits the camber of the wings. Aerodsn requires an axis-symmetric vehicle and using camber is not allowed in Aerodsn. Future improvements will allow for different wing configurations and for camber to be used.

The diameter of the 1st stage must be equal to or greater than the diameter of the 2nd or 3rd stages. For the Minuteman-III, the 2nd and 3rd stage diameters are equal. For the first study, the stage diameters are set to the Minuteman-III value. The second study allows the 3rd stage diameter to be smaller than the 2nd stage diameter for the generic three-stage vehicle. The aerodynamics model is initially called before liftoff with all the

stages stacked together, and then it is called after stage 1 burnout, after stage 2 burnout, and after stage 3 burnout. Essentially, the aerodynamic properties are calculated every time the vehicle geometry changes.

The properties calculated by Aerodsn are used in conjunction with the mass properties model to calculate all the aerodynamic forces acting on the vehicle. The aerodynamics of the vehicle is relatively unimportant to this work. The benefit of the lifting wings and the negative of the aerodynamic drag is only a concern during the first stage burn. The explanation for this is explained in more detail at the start of section 4.0.

Mass Properties

The mass properties code is another important piece of the model. The airfoil section for both the wing and tail fin sets are assumed to be circular arc airfoils. It is assumed that the wing has no camber and that the leading and trailing edges are identical. A generic circular arc cross-section is shown in Figure 7.

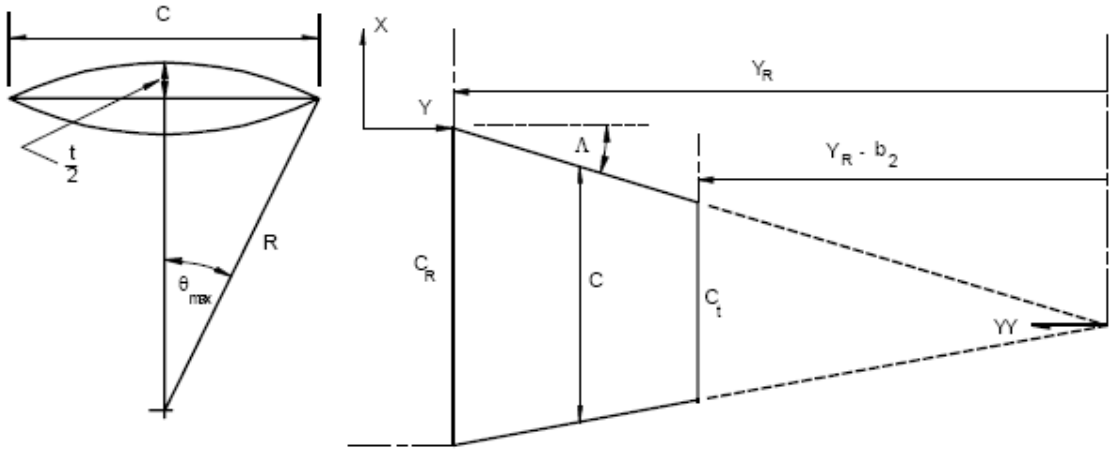

Figure 7: Circular Arc Airfoil[30]

The following equations are adapted from Ref. 30. The radius of the fin and the angle θ_{max} are expressed by

$$R = \frac{1}{4}\left[\frac{c}{t} + \frac{t}{c}\right]\left[\frac{C_R - C_t}{b/2}\right] yy = R_{const}\, yy \qquad (15)$$

$$\theta_{\max} = \sin^{-1}\left(\frac{C}{2R}\right) \qquad (16)$$

The cross-sectional area of the fin can be expressed as

$$Area = \left[2(R_{const})^2 \theta_{\max} - R_{const}\left(\frac{C_R - C_t}{b/2}\right)\cos(\theta_{\max})\right] yy^2 = (A_{const})yy^2 \qquad (17)$$

The mass of the fin is thus expressed as

$$m = \frac{\rho A_{const}}{3}\left[y_R{}^3 - \left(y_R - b/2\right)^3\right] \qquad (18)$$

The mass of the vehicle is not constant because it burns and ejects propellant during flight. The mass properties code calculates the mass, products of inertia, and x-center of gravity for every individual component. The axi-symmetric configuration of the vehicle reduces the products of inertia to zero. The mass properties model is described in detail in Ref. 3, and except for the addition of wing fins and tail fins remains unmodified for this study; however it is relevant to list the five mass properties that are calculated by this model[3]:

1. Mass of each individual component and entire launch vehicle system
2. Center of gravity relative to the nose of the rocket (xcg) of the individual component and the entire launch vehicle system
3. X-axis moment of inertia (ixx) of the individual component and entire system

4. Y-axis moment of inertia (iyy) of the individual component and entire system

5. Z-axis moment of inertia (izz) of the individual component and entire system

The components that are analyzed by the mass properties code for the three-stage launch vehicle are shown in Table 6.

Table 6: Mass Property Components

System Components	Stages 1-2-3	Stage 1
Blunt Nose	Bulkhead	Wings
Ogive	Ignitor	Tails
Payload	Motor Case	
Electronics	Liner	
	Insulation	
	Nozzle	
	Propellant Grain	

Dynamics Simulation

The six degree of freedom model (six-DOF) is the core analysis tool used to determine performance. All the performance characteristics are calculated inside the six-DOF. The six-DOF code can be considered the 'project manager' of the predictive model. The digital flight of the model is initiated and completed using a 7-8th order Runge-Kutta integration routine (RK78). The RK78 routine integrates the equations of motion. The propulsion, mass properties, and aerodynamics models are all called from the six-DOF to update parameters real-time during the flight. The integration process continues until the vehicle reaches the apogee of the ballistic flight trajectory. The apogee ideally corresponds to the orbital insertion point for a low-Earth, circular orbit. Once the six-DOF is complete, the desired goals such as orbital altitude and orbital velocity are sent to the genetic algorithm for analysis. The goal of the optimization is to minimize the values obtained from the six-DOF with the desired values that are set prior to the analysis.

3.0 VALIDATION

To be useful as design tools, computer models of physical systems require proof of the validity of the physical model. Validation is the process of determining if the physical system being modeled is correct. A validated model provides a degree of confidence in the accuracy of the physical system and the results from an optimization study which uses the model.

Individual components of the predictive model used in the current study have been validated independently in previous studies. The solid propellant propulsion model was developed and validated by Burkhalter[28], Hartfield[30], and Sforzini[31]. The aerodynamics model, Aerodsn, has been an industry tool since 1990. Aerodsn and the six-DOF flight dynamics simulator have been used and validated extensively by Hartfield et al[15,16,17].

The three-stage solid-fuel orbital flight model for this thesis was validated using real world data for the Minuteman-III ICBM[32,33]. The Minuteman-III is a strategic weapon system using a ballistic missile of intercontinental range. Although the Minuteman-III was not designed to take a payload into orbit, it was chosen for this study because it has a known configuration that reaches suborbital altitude and velocity. Using the known data for the Minuteman-III, the GA is used to determine the unknown parameters. An optimization is performed to develop a vehicle having similar characteristics to the real-world example. If the model can produce a vehicle with very

similar parameters to the real vehicle, then the validity and uncertainty of the model can be ascertained.

This validation effort was a repeat of a previous effort by Bayley[3] and had identical results. Bayley's validation effort was reported here due to changes made in the program. Table 7 shows the results of the validation.

Table 7: Minuteman-III Validation

Parameter	Model	Minuteman III ICBM
Payload*	2,540.00 lbm	2,540.00 lbm
Initial Vehicle Weight	75,870.09 lbm	79,432.00 lbm
Total Vehicle Length	61.33 ft	59.90 ft
Final Altitude	763,306.27 ft	750,000.00 ft
Final Velocity	22,071.61 ft/s	22,000.00 ft/s
Stage 1		
Stage Length*	295.20 in	295.20 in
Stage Diameter*	66.00 in	66.00 in
Propellants*	PBAA/AP/Al	PBAA/AP/Al
Total Stage Weight	49,881.91 lbm	50,485.84 lbm
m_{prop}	45,853.21 lbm	45,371.21 lbm
m_{inert}	4,028.70 lbm	5,114.64 lbm
f_{prop}	0.9192	0.8987
Burnout Time	67.72 s	61.00 s
Burnout Altitude	119,785.81 ft	100,000.00 ft
Stage 2		
Stage Length*	184.00 in	184.00 in
Stage Diameter*	52.00 in	52.00 in
Propellants*	PBAA/AP/Al	PBAA/AP/Al
Total Stage Weight	15,514.05 lbm	15,432.35 lbm
m_{prop}	13,993.11 lbm	13,668.69 lbm
m_{inert}	1,520.94 lbm	1,763.67 lbm
f_{prop}	0.9020	0.8857
Burnout Time	130.32 s	126.00 s
Burnout Altitude	406,211.02 ft	300,000.00 ft
Stage 3		
Stage Length*	90.00 in	90.00 in
Stage Diameter*	52.00 in	52.00 in
Propellants*	PBAA/AP/Al	PBAA/AP/Al
Total Stage Weight	7,665.72 lbm	9,520.00 lbm
m_{prop}	6,897.00 lbm	7,054.80 lbm
m_{inert}	768.72 lbm	881.83 lbm
f_{prop}	0.8997	0.8889
Burnout Time	189.23 s	191.00 s
Burnout Altitude	763,306.27 ft	750,000.00 ft
Burnout Velocity	22,071.61 ft/s	22,000.00 ft/s

Values in Table 7 listed in bold* were direct inputs based on known Minuteman-III data. The rest of the parameters were determined by the GA. The results of the GA optimization are very close to the published Minuteman-III data. An important validation check is in the ability of the model to reproduce the performance characteristics such as the final altitude (763,306.27 ft to 750,000.00 ft) and burnout velocity (22,071.61 ft/s to 22,000.00 ft/s). Stage weights burnout times match fairly closely as well. This validation was performed with no wings and tails. Coincidently, an optimization case performed for this study (discussed in section 4) that includes wings and tails was able to narrow down on the altitude and velocity values by a large margin while only changing the system mass by a negligible amount. Figure 8 shows a diagram of the validation vehicle next to a photo of the physical Minuteman-III.

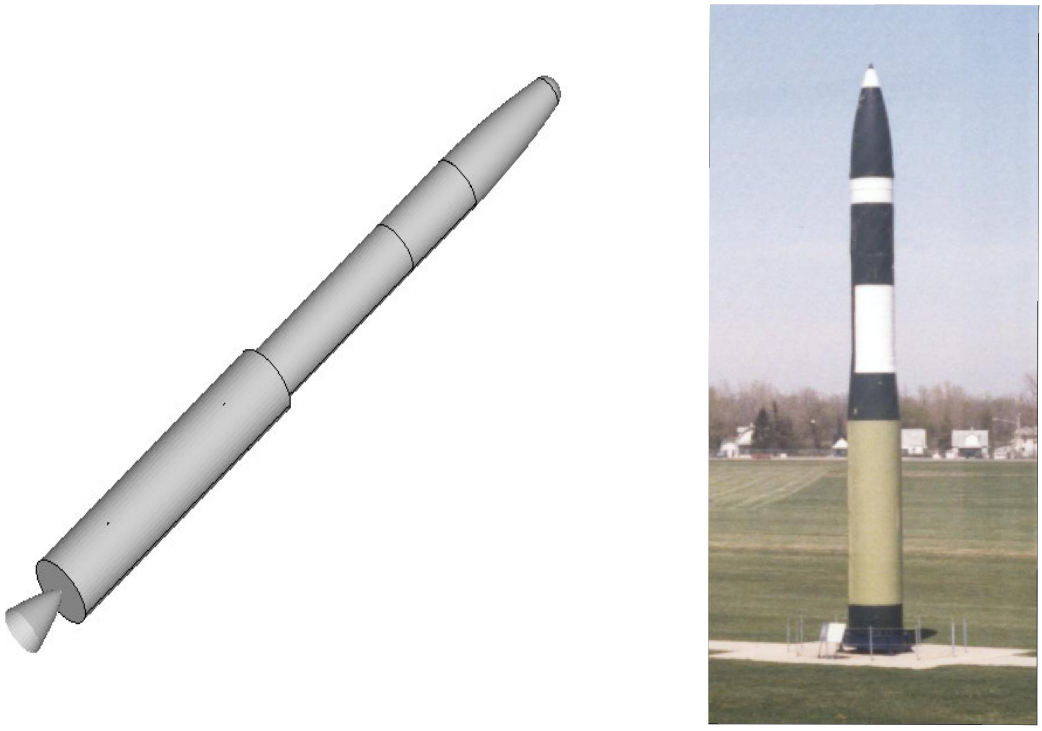

Figure 8: Minuteman-III Validation Model

The fuel for each stage is PBAA/AP/Al. Table 8 shows a list of the characteristics of the propellant.

Table 8: PBAA/AP/Al Characteristics (English Units)

Parameter	Value
a	0.0285
n	0.35
rho	0.064
Tc	6159.67
gamma	1.24
cstar	5700
Tio	519
MW	24.7

An important parameter to compare vehicles is the propellant mass fraction calculated by

$$f_{prop} = \frac{m_{fuel}}{m_{fuel} + m_{inert}} \tag{19}$$

The vehicles with wings should have a smaller propellant mass fraction than the vehicles without wings.

4.0 AERODYNAMIC PERFORMANCE ENHANCEMENT

As discussed in section 1.0, it is very likely that substantial improvement in net payload to orbit could be obtained for current launch vehicles using aerodynamic lifting during the first stage burn despite the cost of adding some mass in the form of wing structure (to the first stage). Attaching the wing structure to the first stage makes the most use of any possible aerodynamic lifting effects. As the vehicle climbs in altitude, the density of the air molecules drastically decreases. The flight envelope where aerodynamic forces are non-trivial is limited to the first-stage portion of the trajectory due to the decrease in density. Figure 9 shows graphically how density decreases as altitude increases. At 100,000 feet, the density is 1% of the sea-level value.

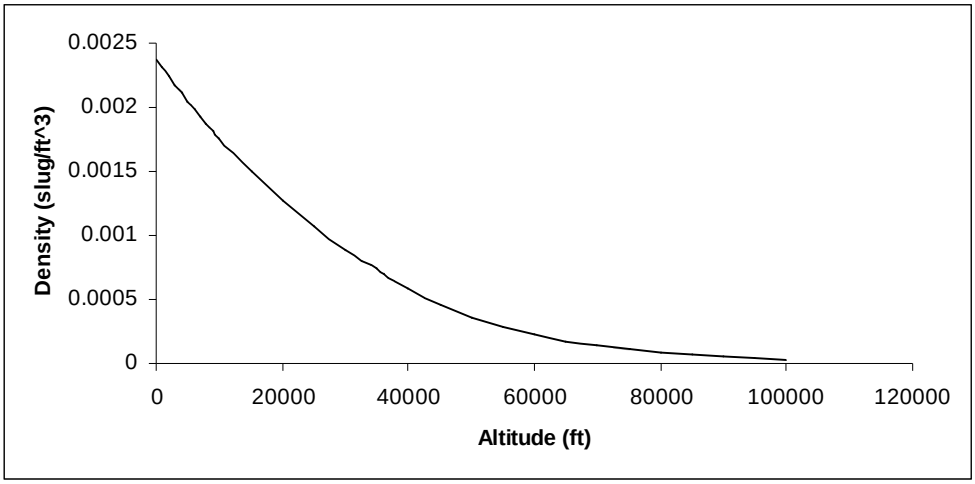

Figure 9: Air Density vs. Altitude

Another important parameter for spacecraft is the dynamic pressure because it can show the point of maximum aerodynamic load on the vehicle. Dynamic pressure is described by equation 19. Figure 10 shows the dynamic pressure for the first stage flight of the Minuteman-III.

$$Q = \frac{1}{2}\rho V^2 \tag{19}$$

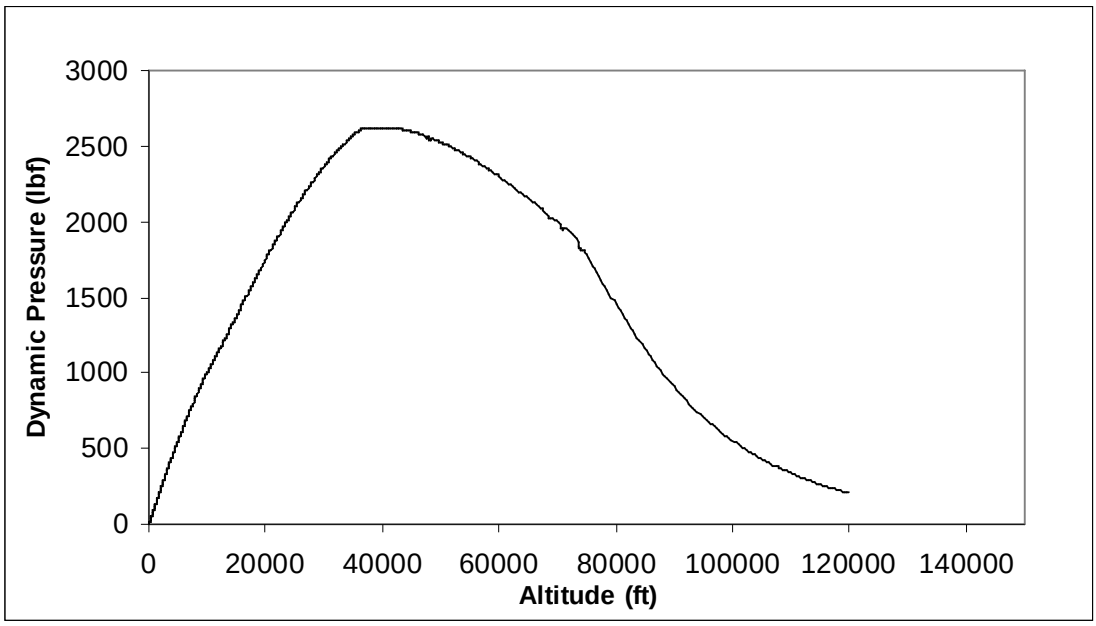

Figure 10: Minuteman-III Dynamic Pressure

The performance enhancement revolves around the wing and tail configuration. A rocket with no fins is unstable, so fins are attached in order to aerodynamically stabilize the vehicle at a specific trim angle. One of the purposes for the optimization studies presented herein is to use the genetic algorithm to find a fin configuration that enables the rocket to trim at a higher angle of attack. At the higher trim angle, the body and fin system will have a higher normal force than the body alone. The trim angles for the vehicles in this study range from slightly above 0 degrees to a maximum of 4.3 degrees.

Performance enhancement testing is divided into three groups with all tests employing the wing and tail system. The propellant type is a constant and therefore is the same for every optimization study. First, the Minuteman-III external body geometry is kept constant to the validation model except for the addition of a wing and tail system. Three optimization tests are performed on this configuration with a desired suborbital altitude of 750,000 feet and velocity of 22,000 ft/s:

1. The payload and propellant fuel mass are held constant.
2. The payload is increased by 10% for a system with wings and for the validation system.
3. For both payloads, the desired propellant fuel mass and the desired initial system weight are reduced.

Second, the three-stage Minuteman-III geometry is used to attempt to achieve low-earth orbit conditions of 2,430,000 feet and 24,550 ft/s with a payload of 1,000 pounds. Tests are conducted with the validation Minuteman-III system (no wings) and compared to an enhanced Minuteman-III configuration equipped with the wing and tail system.

The third group of tests compares the result of a generic three-stage launch vehicle optimization performed by Bayley[3] to the result of the same optimization procedure using the wing and tail system.

4.1 MINUTEMAN-III SUBORBITAL ENHANCEMENT

The Minuteman-III (Figure 11) is a three-stage solid ICBM and achieves a suborbital apogee of 750,000 feet and a speed of 22,000 ft/s. The payload is 2,540

pounds. The predictive model successfully validated a Minuteman-III vehicle as seen in section 3. Analysis of this system is divided into two groups: Improving the suborbital flight, and taking the MM3 to full orbital conditions.

Figure 11: Minuteman-III

Four cases were studied to improve the suborbital flight, and one to take the three-stage system to orbit.

4.1.1 SUBORBITAL IMPROVEMENT

The first suborbital test was to improve on the performance (matching the desired altitude and velocity) of the validation case by keeping the external geometry, propellant type, and payload the same, but adding wings and tails to the first stage. The design variables are the geometric definition of the wing and tail (Table 4) and the internal geometry of the propellant. The optimized vehicle is shown in Figure 12.

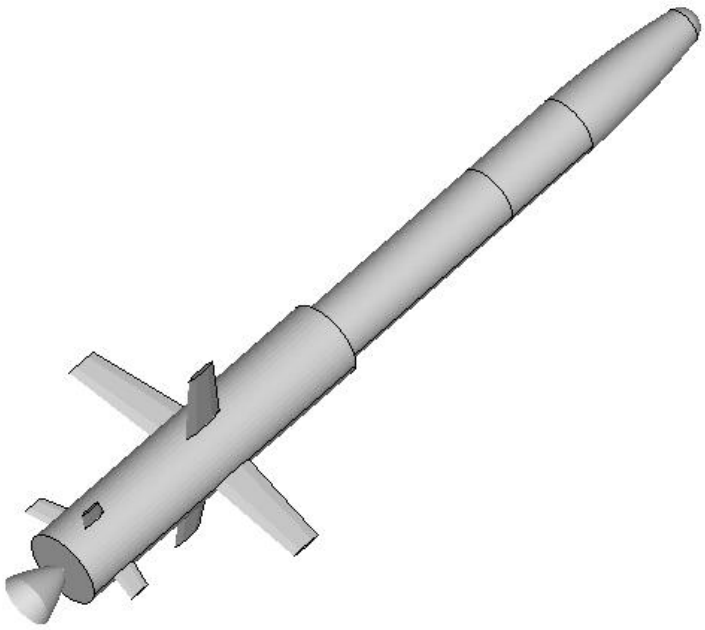

Figure 12: Minuteman-III with 2540 Payload

The wings presented for this vehicle are unrealistic, but serve as a proof of concept for the idea of enhancing performance through aerodynamic assistance. With a more accurate structural analysis, the wings presented here would break off under the load. An improvement to the model for future analysis should include more restrictions

on the semi-span and chord length to limit the aspect ratio. All the suborbital enhancement cases have this issue. In addition, the model does not show fairings over the variable diameter stage connections. The model contains a correction factor for the drag computations.

The new vehicle weighed less and matched the desired values for altitude and velocity much more closely than the original validation. This vehicle attained an altitude of 750,007 ft, a speed of 22,000.8 ft/s, and total system mass of 74,935 lbm. Noticing that this vehicle flies to 750,007 ft and the validation model flies to 763,306 ft, it is possible that the mass savings could be due in part to the vehicle flying to a lower altitude. However, the remaining test cases also closely match the desired altitude, and the initial mass is shown to be further reduced when compared to the previous case.

The additional control provided by the wing and tail system allowed the trajectory to more closely match the desired suborbital values than the original validation case. The ballistic trajectory can be seen in Figure 13, the thrust profile in Figure 14, and the velocity profile in Figure 15.

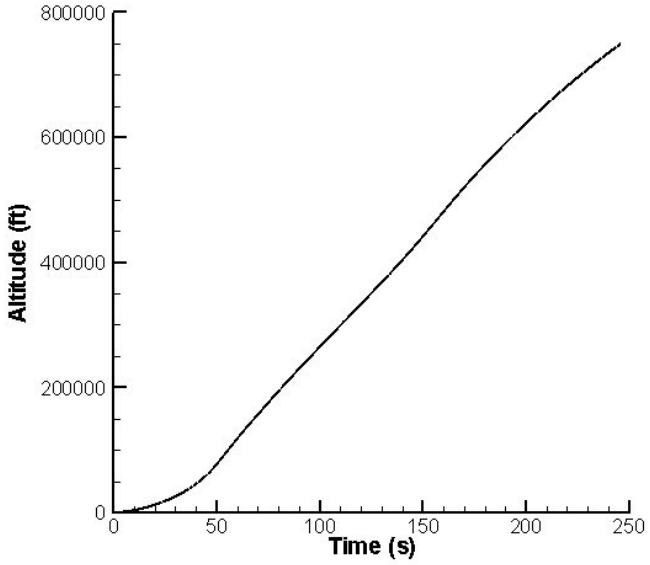

Figure 13: Altitude vs. Time (MM3-Wings)

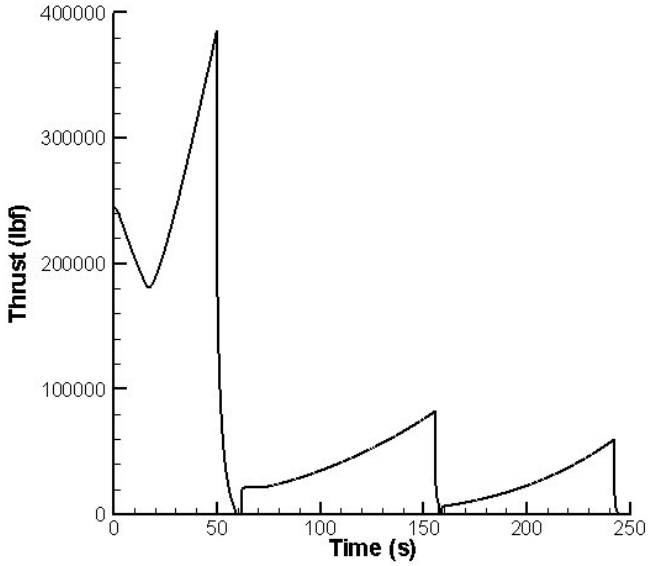

Figure 14: Thrust vs. Time (MM3-Wings)

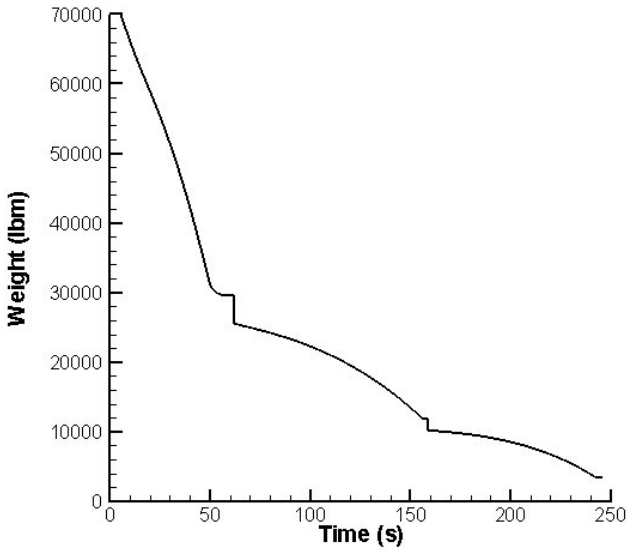

Figure 15: Weight vs. Time (MM3-Wings)

Figure 15 displays how the weight of the system decreases with time. The smooth curves are the loss in weight caused by the burning propellant. The points where the vehicle disposes of a used stage are clearly seen. The first drop off is the largest in mass and includes the first stage and the wing structure. The genetic algorithm convergence to the optimal solution can be seen in Figure 16. The optimization was carried out for 400 generations, hit a plateau at generation 60 but improved again near generation 300.

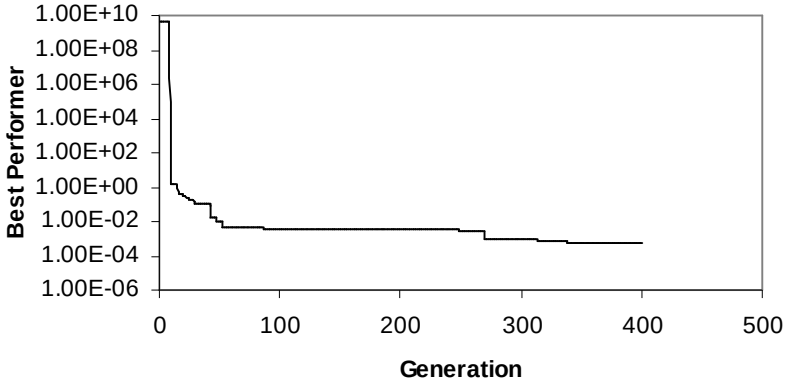

Figure 16: GA Best Answer Convergence

The next suborbital test case kept the payload (2,540 lbm) and external geometry constant but reduced the desired first stage fuel mass by 5.2% from 45,371 pounds to 43,000 pounds. A reduction in propellant translates into a direct reduction in costs. Again, the only variables are the wing and tail definitions and the internal propellant geometry. Figure 17 shows a diagram of the optimized vehicle. This vehicle has a 74 degree launch angle and attains an altitude of 749,992.6 feet, a velocity of 22,000.0 ft/s, and weighs 72,402 pounds. This vehicle weighs 2,533 pounds less than the previous case. From the previous design, the wings have progressed towards a more aerodynamic efficient shape. The new, thinner shape of the wings has a lower induced drag. As will be seen in subsequent diagrams, the general trend of evolution using the genetic algorithm is that thinner wings are designed for the vehicles having the lowest initial system mass. The previously mentioned issues concerning the unrealistic wings apply to this case. These wings would break if the structural model was more accurate. Genetic algorithm best performer convergence is shown in Figure 18.

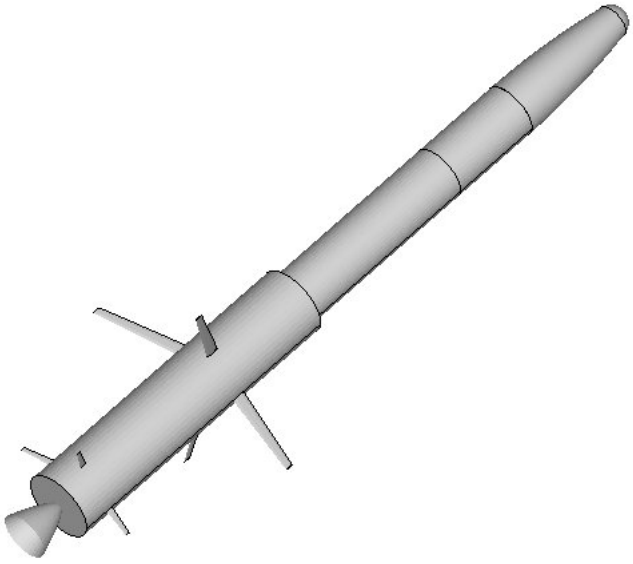

Figure 17: Vehicle Diagram (MM3-Reduced Propellant)

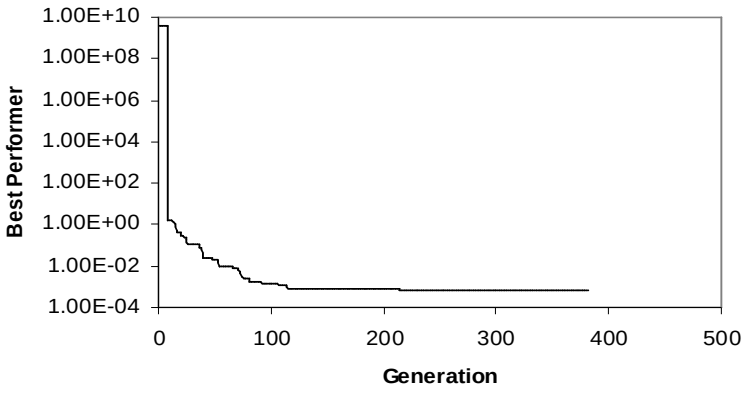

Figure 18: Convergence for MM3-Reduced Propellant

The next test to improve the suborbital performance of the Minuteman-III was to increase the payload by 10%, from 2540 pounds to 2794 pounds, with a negligible increase in the initial system mass. The design variables are the wing and tail definitions and the internal propellant geometry. The optimization produced a vehicle that matched the desired goals closely and had an initial system mass of only a fraction more. The

vehicle is seen in Figure 19 and weighs 74,959 pounds, is launched at 71 degrees, reaches an altitude of 749,997.5 feet, and reaches a speed of 22,000.2 ft/s. The structural issues for the wings apply to this case. Future investigations will limit the aspect ratio further to prevent this problem.

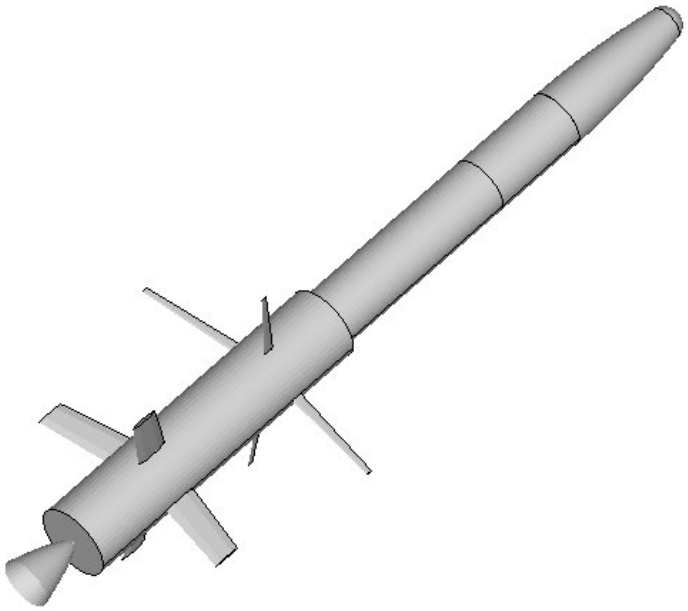

Figure 19: Vehicle Diagram (MM3-Increased Payload)

The convergence of the best performer is similar to the previous test cases, reaching an optimum solution around the 60th generation and improving only slightly afterwards.

As a comparison to the previous case, the analysis that produced the Minuteman-III validation model (no wings) was performed using the increased payload of 2,794 pounds. This optimization case produced a vehicle that reaches an altitude of 749,998 feet, a speed of 22,000.1 ft/s, and weighs 77648.2 pounds. The original MM3 validation

weighed 75,807.09 pounds, leading to an increase of 1841.11 pounds in order to increase the payload by 10%. The previous case with the wing structure only increased the system mass by 24 pounds when the payload was increased.

Table 9: MM3 Suborbital Enhancement

Case	Wings	Payload (lbm)	Weight (lbm)	Altitude (ft)	Velocity (ft/s)
Validation Model	No	2,540	75,870	763,306	22,071
Enhancement 1	Yes	2,540	74,935	750,007	22,001
Enhancement 2	Yes	2,540	72,402	749,993	22,000
Validation Model	No	2,794	77,648	749,988	21,997
Enhancement 3	Yes	2,794	74,959	749,998	22,000

Table 10: MM3 Suborbital Mass Fractions

Case	f_{prop}
Validation Model	0.9102
Enhancement 1	0.9095
Enhancement 2	0.9070
Validation Model	0.9123
Enhancement 3	0.9068

Table 9 shows a summary of the basic performance characteristics for all the suborbital performance enhancement cases that were studied. Analyzing the weight column, it can be seen that all the cases that include the wing structure have lower initial weights than the cases without wings. Also, increasing the payload by 10% increased the initial weight of the validation case by a much larger amount than for the case with wings (Enhancement 3). Table 10 shows the propellant mass fractions for each case. The vehicles with no wings have a higher propellant mass fraction than the vehicles with wings. This shows that when using the wings, a smaller amount of propellant is needed. These studies serve as a proof of concept that the suborbital flight performance of the Minuteman-III can be improved through aerodynamic lifting on the first stage.

4.1.2 ORBITAL IMPROVEMENT

The Minuteman-III is not an orbital vehicle, but tests were conducted to determine if the Minuteman-III geometry from the validated model could sustain a flight to orbital conditions. After a successful design to orbit, a second test was performed with the goal of enhancing performance through aerodynamic lifting during the first stage burn. This section discusses these tests and compares the results.

The first test was to take the validation model to orbit. The desired goals were changed from suborbital conditions to a desired altitude of 2,430,000 feet and desired velocity of 24,550 ft/s. The payload was changed from the Minuteman-III suborbital value of 2,540 pounds to a more typical orbital payload of 1,000 pounds. As before, the only variables that are allowed to change are the wing and tail geometry definitions and the internal propellant geometry. The genetic algorithm was able to converge to a design that achieved the desired orbital conditions, reaching an altitude of 2,430,024 feet and a velocity of 24,551 ft/s. The diagram of the vehicle is the same as previous Minuteman-III validation configurations (such as Figure 8) because the external geometry is constant.

The vehicle weighs 75,760 pounds, which is similar to the 75,870 pounds that the validation case weighs to reach suborbital conditions. This vehicle is 110 pounds lighter than the validation case yet achieves a higher altitude and faster velocity. The 1,540 pound reduction in payload was directly applied to the first and second stage propellant mass. The validation case had a first and second stage propellant mass of 45,371 pounds and 13,668 pounds respectively, and the current vehicle has first and second stage propellant mass of 46,750 pounds and 14,413 pounds respectively. Figure 20 shows the

genetic algorithm convergence history of the best performer. Similar to the previous convergence plots shown, a near-best solution is found around generation 60, and is refined over the course of the rest of the generations.

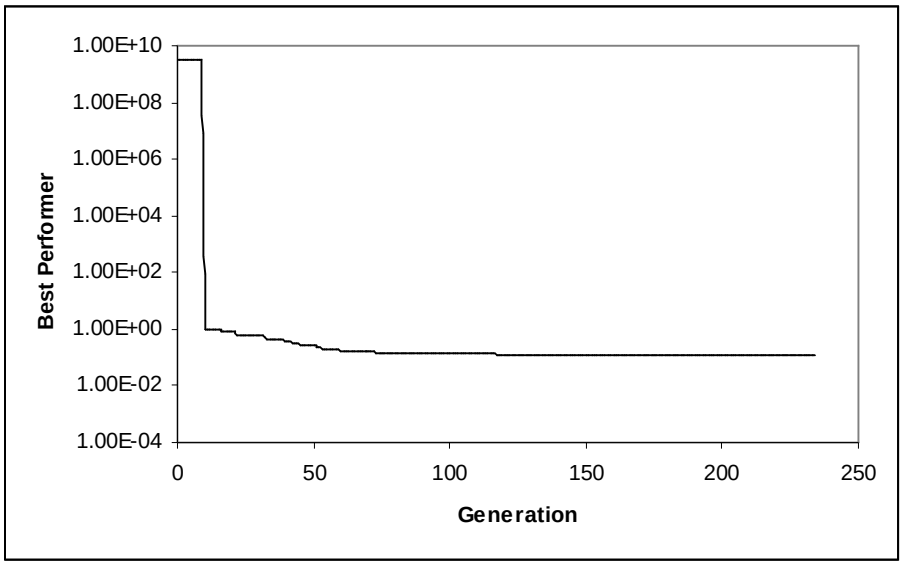

Figure 20: Orbital MM3 GA Convergence

The next case attempts to take the Minuteman-III geometry with the wing structure to the same orbital conditions as the previous case. The vehicle chosen as the best performer achieves an altitude of 2,429,956 feet and a velocity of 24,551 ft/s. The initial system weight is 75,486 pounds, only 274 pounds lighter than the previous MM-3 vehicle. The mass of the propellant is slightly less than the previous vehicle, with 46,557 pounds for the first stage and 14,311 pounds for the second stage. The small wings make a very slight improvement for this case. Figure 21 shows a diagram of this vehicle. Figure 22 shows the altitude versus time plot, Figure 23 shows the thrust profile, and Figure 24 shows the convergence history.

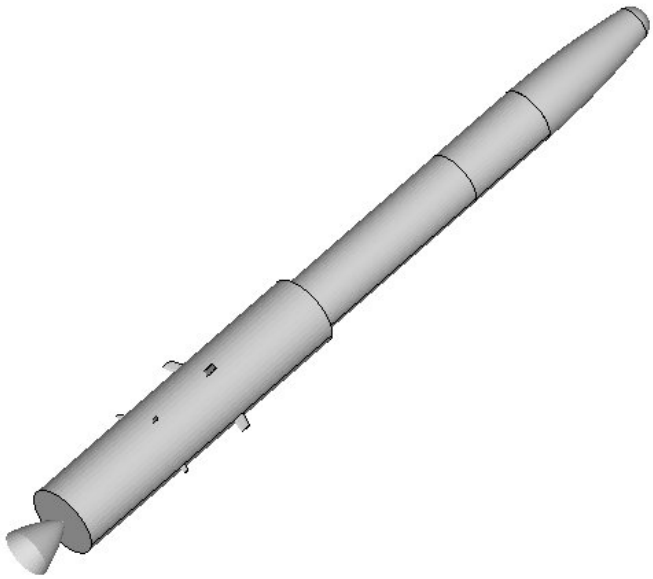

Figure 21: Orbital MM3 Wings

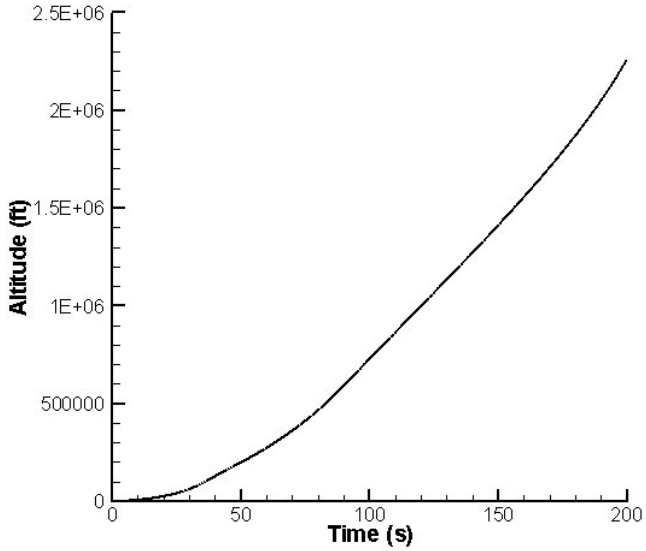

Figure 22: Orbital MM3 Altitude vs. Time

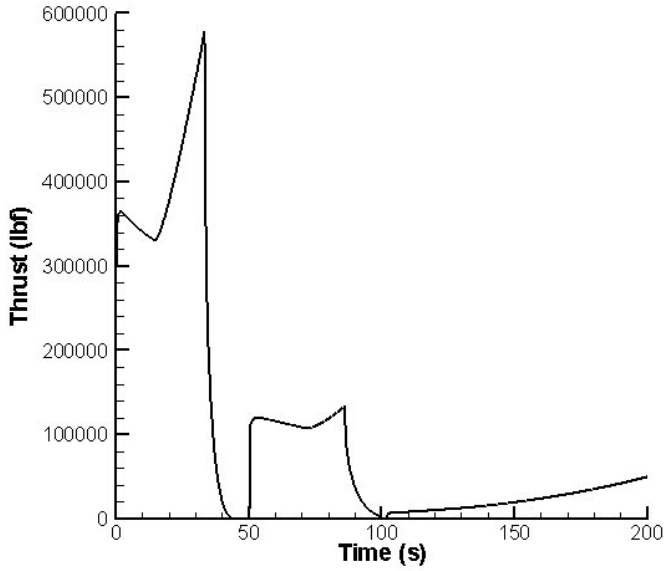

Figure 23: Orbital MM3 Thrust Profile

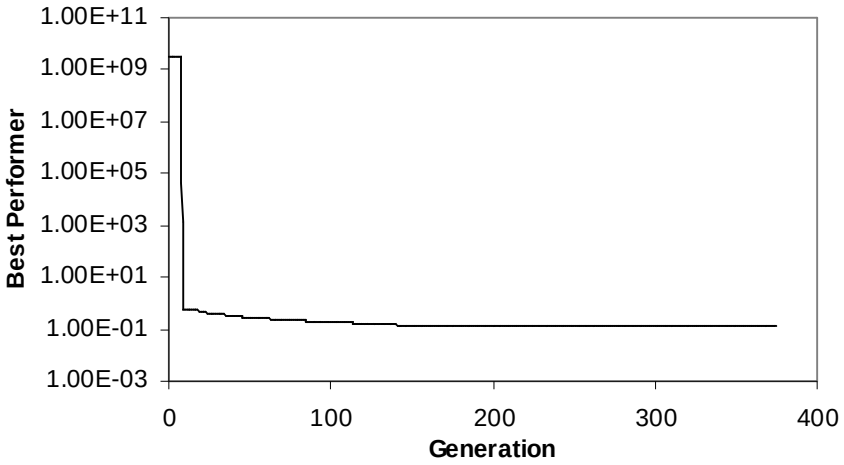

Figure 24: Orbital MM3 Convergence History

Table 11 summarizes the performance goals of the two orbital designs.

Table 12 shows the propellant mass fractions for these two vehicles. The propellant mass

fractions are very similar, and the fraction for the vehicle with wings is only slightly smaller than for the vehicle without wings.

Table 11: MM3 Orbital Enhancement

Case	Wings	Payload (lbm)	Weight (lbm)	Altitude (ft)	Velocity (ft/s)
Validation Model	No	1,000	75,760	2,430,024	24,551
Enhancement 1	Yes	1,000	75,486	2,429,956	24,551

Table 12: MM3 Orbital Mass Fractions

Case	f_{prop}
Validation Model	0.91313
Enhancement 1	0.91302

4.2 THREE-STAGE ORBITAL ENHANCEMENT

The generic three-stage solid fuel model includes more variables than the validation model. The stage lengths and stage diameters are not hard-wired to match the Minuteman-III and are included in the design space for the GA. Wall thickness parameters were known for the MM3 but are calculated for the generic model, therefore the initial system weight is on a different scale than for the MM3 cases. Due to this discrepancy, the comparisons for vehicles with the wing structure to a baseline case are done using the optimizations performed by Bayley[3]. The same design optimizations are performed but with the addition of the wing structure and the results are compared.

The baseline vehicle attains an altitude of 2,439,276 feet, a velocity of 24,595 ft/s, and has an initial system mass of 89,906 pounds. The specific details of the flight can be seen in Ref. 3. The wing structure was added to this model and the optimization performed again. The same wing and tail variables that were added to the Minuteman-III,

seen in Table 4, are added to the generic three-stage model. The result of this optimization is a much lighter vehicle. The desired goals are matched well. The vehicle attains an altitude of 2,429,965 feet and a velocity of 24,550 ft/s. The initial system mass of the vehicle dropped from 89,906 pounds to 80,002 pounds. Figure 25 shows a diagram of the vehicle.

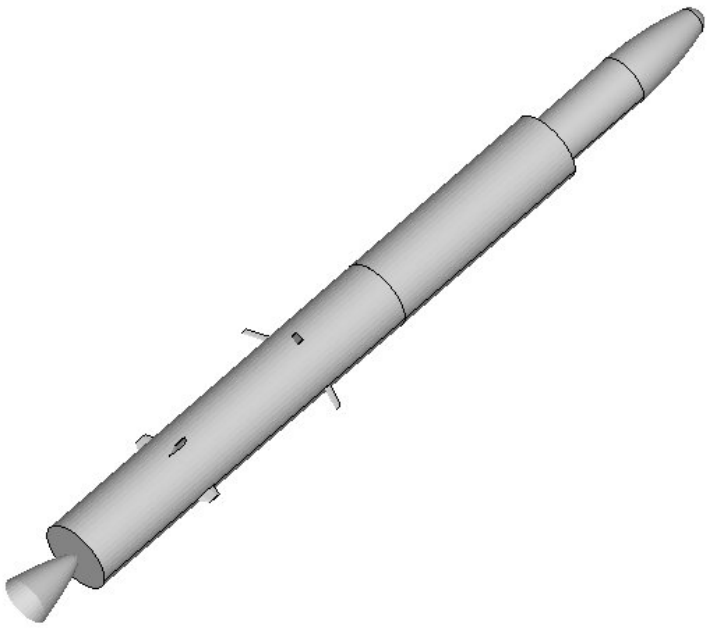

Figure 25: Generic Three-Stage Vehicle

The first stage propellant mass dropped from 48,939 pounds to 45,002 pounds. The second stage propellant mass dropped from 18,965 pounds to 17,029 pounds. The altitude plot and thrust profile are shown in Figure 26 and Figure 27.

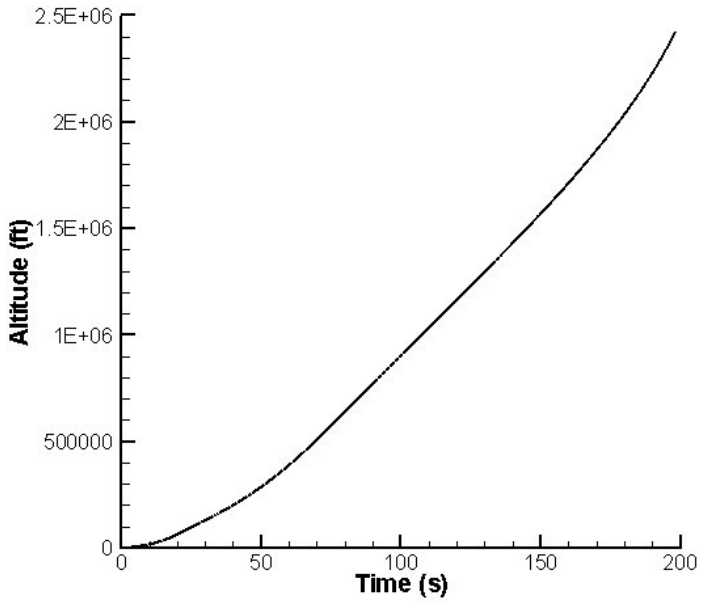

Figure 26: Three-Stage Altitude vs. Time

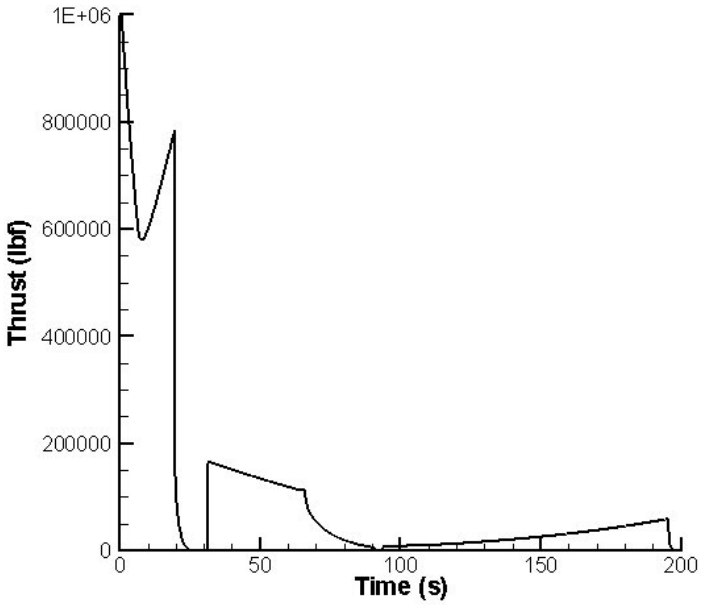

Figure 27: Three-Stage Thrust Profile

Table 13 shows a summary of the performance goals for the generic three-stage vehicles.

Table 13: Generic Three-Stage Orbital Enhancement

Case	Wings	Payload (lbm)	Weight (lbm)	Altitude (ft)	Velocity (ft/s)
3-Stage	No	1,000	89,906	2,439,276	24,595
3-Stage Enhance	Yes	1,000	80,002	2,429,965	24,550

Table 14: Generic Three-Stage Mass Fractions

Case	f_{prop}
3-Stage	0.9078
3-Stage Enhance	0.8904

Table 14 shows the propellant mass fractions for the generic three stage optimizations. The vehicle with the wings has a slightly lower propellant mass fraction than the vehicle without wings.

5.0 SUMMARY

Launch vehicle performance enhancement using aerodynamic assistance during early flight has proven to be successful for the current design models. The Minuteman-III suborbital performance was shown to improve by using a wing and tail system. It was shown that by only changing the geometric definition of the wings, tails, and propellant geometry the payload could be increased by 10% with no increase in the initial total system mass. It was also shown that the first stage propellant mass could be decreased while achieving the same performance parameters using the winged vehicle. Every comparison case of the baseline Minuteman-III to a version with wings showed that the vehicle with wings had a lower initial system weight.

The impact of the wings was not as large when the Minuteman-III was changed from a suborbital flight to an orbital flight. The MM3 external geometry is locked in, so the only way to improve the performance is by using fins to increase the trim angle, modifying the propellant geometry, and varying the launch angle. With an orbital altitude of 2,430,000 feet (compared to the suborbital altitude of 750,000 feet) and a ballistic trajectory, the required launch angle was 89 degrees. This left little room for the wings to have a large effect on the performance. It was shown that there is a total weight savings even with the launch angle at 89 degrees, but it was not as large as for the suborbital flights.

The non-optimized generic three-stage solid fuel vehicle showed a big weight savings, a little over 11%, when using wings. The small effect of the wings allowed the first, second, and third stage geometries and propellant grains to be redesigned significantly and this all contributed to the weight reduction.

This study indicates that performance enhancement through aerodynamic assist on launch vehicles is a valid proposal and warrants subsequent studies. There are several improvements that should be undertaken for future work. While the current model calculates the weight of the wings, it does not model the support structure in detail. To more accurately represent the total weight penalty for adding wings, the support structure should be modeled structurally to ensure adequate structural integrity of the entire vehicle. Additionally, improved fin settings could be introduced in order to change the angle of attack of the wings during flight. A trajectory modification is recommended for the future. The current trajectory is non-guided and follows a mostly ballistic path. A guided trajectory is suggested for study in order to have a trajectory where the vehicle is kept for a longer period of time in the flight envelope for aerodynamic assistance. Another improvement is to modify the Aerodsn package to allow for non-cruciform fin configurations to be analyzed.

Additional improvements could include more detailed modeling of the aerodynamic effects during the atmospheric flight, the addition of a gimbaled control system and higher fidelity modeling of the entire structure. For a more comprehensive preliminary design study to look at proposed new launch vehicle applications, more modern propellants should be considered along with winged liquid propellant two stage systems.

REFERENCES

1. Lyons, J. T.; Woltosz, W. S.; Abercrombie, G. E.; Gottlieb, R. G NASA-CR-129000, TR-243-1078, 1972.
2. Woltosz, W., Personal Communication.
3. Bayley, D., Hartfield, R.J., Burkhalter, J.E., and Jenkins, R.M., "Design Optimization of a Space Launch Vehicle Using a Genetic Algorithm," AIAA Paper 2007-1863, presented at the 3rd AIAA Multidisciplinary Design Optimization Specialist Conference, Honolulu, Hawaii, April 23-26, 2007.
4. Holland, J. H., *Adaptation in Natural and Artificial Systems*, The University of Michigan Press, Ann Arbor, MI, 1975.
5. Burger, C. and Hartfield, R.J., "Propeller Performance Optimization using Vortex Lattice Theory and a Genetic Algorithm", AIAA-2006-1067, presented at the Forty-Fourth Aerospace Sciences Meeting and Exhibit, Reno, NV, Jan 9-12, 2006.
6. Doyle, J., Hartfield, R.J., and Roy, C. "Aerodynamic Optimization for Freight Trucks using a Genetic Algorithm and CFD", AIAA 2008-0323, presented at the 46th Aerospace Sciences Meeting and Exhibit, Reno, NV, January 2008.
7. Anderson, M.B., "Using Pareto Genetic Algorithms for Preliminary Subsonic Wing Design", AIAA Paper 96-4023, presented at the 6th AIAA/NASA/USAF Multidisciplinary Analysis and Optimization Symposium, Bellevue, WA, September 1996.

8. Oyama, A., Obayashi, S., Nakahashi, K., “Transonic Wing Optimization Using Genetic Algorithm”, AIAA Paper 97-1854, 13th Computational Fluid Dynamics Conference, June 1997.
9. Jang, M., and Lee, J., “Genetic Algorithm Based Design of Transonic Airfoils Using Euler Equations”, AIAA Paper 2000-1584, Presented at the 41st AIAA/ASME/ASCE/AHS/ASC Structures, Structural Dynamics, and Materials Conference, April 2000.
10. Jones, B.R., Crossley, W.A., and Anastasios, S.L., “Aerodynamic and Aeroacoustic Optimization of Airfoils Via a Parallel Genetic Algorithm”, AIAA Paper 98-4811, 7th AIAA/USAF/NASA/ISSMO Symposium on Multidisciplinary Analysis and Optimization, September 1998.
11. Schoonover, P.L., Crossley, W.A., and Heister, S.D., “Application of Genetic Algorithms to the Optimization of Hybrid Rockets”, AIAA Paper 98-3349, 34th AIAA/ASME/SAE/ASEE Joint Propulsion Conference and Exhibit, July 1998.
12. Nelson, A., Nemec, M., Aftosmis, M., and Pulliam, T., “Aerodynamic Optimization of Rocket Control Surfaces Using Cartesian Methods and CAD Geometry,” AIAA 2005-4836, 23rd Applied Aerodynamics Conference, Toronto, Canada, June 6-9, 2005.
13. Anderson, M.B., Burkhalter, J.E., and Jenkins, R.M., "Design of an Air to Air Interceptor Using Genetic Algorithms", AIAA Paper 99-4081, presented at the 1999 AIAA Guidance, Navigation, and Control Conference, Portland, OR, August 1999.
14. Anderson, M.B., Burkhalter, J.E., and Jenkins, R.M., “Intelligent Systems Approach to Designing an Interceptor to Defeat Highly Maneuverable Targets”, AIAA Paper

2001-1123, presented at the 39th Aerospace Sciences Meeting and Exhibit, Reno, NV, January 2001.

15. J.E. Burkhalter, R.M. Jenkins, and R.J. Hartfield, M. B. Anderson, G.A. Sanders, "Missile Systems Design Optimization Using Genetic Algorithms," AIAA Paper 2002-5173, Classified Missile Systems Conference, Monterey, CA, November, 2002.
16. Hartfield, Roy J., Jenkins, Rhonald M., Burkhalter, John E., "Ramjet Powered Missile Design Using a Genetic Algorithm," AIAA 2004-0451, presented at the forty-second AIAA Aerospace Sciences Meeting, Reno NV, January 5-8, 2004.
17. Jenkins, Rhonald M., Hartfield, Roy J., and Burkhalter, John E., **"**Optimizing a Solid Rocket Motor Boosted Ramjet Powered Missile Using a Genetic Algorithm", AIAA 2005-3507 presented at the Forty First AIAA/ASME/SAE/ASEE Joint Propulsion Conference, Tucson, AZ, July 10-13, 2005.
18. Riddle, David B., "Design Tool Development for Liquid Propellant Missile System," MS Thesis, Auburn University, May 10, 2007.
19. Mondoloni, S., "A Genetic Algorithm for Determining Optimal Flight Trajectories", AIAA Paper 98-4476, AIAA Guidance, Navigation, and Control Conference and Exhibit, August 1998.
20. Karr, C.L., Freeman, L.M., and Meredith, D.L., "Genetic Algorithm based Fuzzy Control of Spacecraft Autonomous Rendezvous," NASA Marshall Space Flight Center, Fifth Conference on Artificial Intelligence for Space Applications, 1990.
21. Krishnakumar, K., Goldberg, D.E., "Control System Optimization Using Genetic Algorithms", Journal of Guidance, Control, and Dynamics, Vol. 15, No. 3, May-June 1992.

22. Tong, S.S., "Turbine Preliminary Design Using Artificial Intelligence and Numerical Optimization Techniques", Journal of Turbomachinery, Jan 1992, Vol 114/1.
23. Selig, M.S., and Coverstone-Carroll, V.L., "Application of a Genetic Algorithm to Wind Turbine Design", Presented at the 14th ASME ETCE Wind Energy Symposium, Houston, TX, January 1995.
24. Torella, G., Blasi, L., "The Optimization of Gas Turbine Engine Design by Genetic Algorithms", AIAA Paper 2000-3710, 36th AIAA/ASME/SAE/ASEE Joint Propulsion Conference and Exhibit, July 2000.
25. Koza, J. R., *Genetic Programming*, The MIT Press, Cambridge, MA, 1992.
26. Anderson, M.B., "Users Manual for IMPROVE© Version 2.8: An Optimization Software Package Based on Genetic Algorithms", Sverdrup Technology Inc. / TEAS Group, Eglin AFB, FL, March 6, 2001.
27. Sutton, G., Biblarz, O., *Rocket Propulsion Elements*, John Wiley & Sons, Inc., New York, 2001.
28. Anderson, M.B., Burkhalter, J.E., and Jenkins, R.M., "Multi-Disciplinary Intelligent Systems Approach to Solid Rocket Motor Design, Part II: Multiple Goal Optimization," AIAA Paper 2001-3600, presented at the 37th AIAA/ASME/SAE/ASEE Joint Propulsion Conference and Exhibit, Salt Lake City, UT, July 2001.
29. Hartfield, Roy J., Jenkins, Rhonald M., Burkhalter, John E., and Foster Winfred, "Analytical Methods for Predicting Grain Regression in Tactical Solid-Rocket Motors," Journal of Spacecraft and Rockets, Vol.41 No. 4, July-August 2004, pp.689-693.

30. Burkhalter, J.E., Jenkins, R.M., and Hartfield, R.J., "Genetic Algorithms for Missile Analysis – Final Report", Submitted to Missile and Space Intelligence Center, Redstone Arsenal, AL, 35898, February 2003.
31. Sforzini, R.H., "An Automated Approach to Design of Solid Rockets Utilizing a Special Internal Ballistics Model", AIAA Paper 80-1135, Presented at the 16th AIAA/SAE/ASME Joint Propulsion Conference, July 1980.
32. U.S. Air Force Fact Sheet, LGM-30 Minuteman-III, http://www.af.mil/factsheets/factsheet.asp?id=113
33. System Description of the LGM-30 Minuteman-III, http://www.globalsecurity.org
34. Barrere, M., Jaumotte, A., Veubeke, B.,and Vandenkerckhove, J., *Rocket Propulsion*, Elsevier Publishing Company, Amsterdam, 1960.
35. Huzel, Dieter K. and Huang, David H., *Design of Liquid Propellant Rocket Engines*, Rocketdyne Division, North American Rockwell, Inc, Washington, D.C., 1971 (updated version currently published by AIAA)